Floquet oscillations in periodically driven Dirac systems

Vanessa Junk,[1] Phillipp Reck,[1] Cosimo Gorini,[1] and Klaus Richter[1, *]

[1]*Institut für Theoretische Physik, Universität Regensburg, D-93040 Regensburg, Germany*

Electrons in a lattice exhibit time-periodic motion, known as Bloch oscillation, when subject to an additional static electric field. Here we show that a corresponding dynamics can occur upon replacing the spatially periodic potential by a time-periodic driving: Floquet oscillations of charge carriers in a spatially homogeneous system. The time lattice of the driving gives rise to Floquet bands that, for systems with linear dispersion, take on the role of the usual Bloch bands. For two cases, harmonic driving and periodic kicking through pulses, we numerically demonstrate the existence of such oscillations, both by directly propagating wave packets and based on a complementary Floquet analysis. The Floquet oscillations feature richer oscillation patterns than their Bloch counterpart and enable the imaging of Floquet bands. Moreover, their period can be directly tuned through the driving frequency. Such oscillations should be experimentally observable in effective Dirac systems, such as graphene, when illuminated with circularly polarized light.

Keywords: Floquet, Bloch, Floquet-Bloch oscillations, time periodic systems

In the early days of quantum mechanics, F. Bloch and C. Zener [1, 2] predicted that electrons in a periodic potential, when accelerated by a constant external electric field, perform a time-periodic motion, by now well known as Bloch oscillation [3]. It took about 60 years until this phenomenon was observed in biased semiconductor superlattices [4–7]. Since then Bloch oscillations or analogs of them have been found in various systems ranging from cold atom gases [8, 9] to classical optical [10, 11] and acoustic waves [12], to name a few. In 2014, Bloch oscillations due to the crystal lattice of a biased bulk semiconductor were eventually observed [13].

In the meantime, scientific interest in tuning Bloch bands by means of external time-periodic driving has rapidly grown, especially since the proposal of so-called Floquet topological insulators [14] demonstrating the powerful influence external driving can exert on the properties of a crystal. Recent experiments also showed that Floquet band engineering allows for switching Bloch oscillations on and off [15]. Moreover, additional driving can immensely increase the amplitude of conventional Bloch oscillations, giving rise to "super" Bloch oscillations [16–19].

Here we propose to consider the opposite limit of a time-periodically driven system without any spatial lattice, but still subject to a constant external electric field. We demonstrate that, most notably, still spatially periodic motion of the charge carriers can appear. We call this type of dynamics *Floquet oscillations* since they arise from the periodic repetitions of Floquet quasi-energy bands. So far very few works have addressed Bloch-type oscillations in the absence of an external lattice. One interesting prediction refers to Bloch oscillations of light, i. e. frequency oscillations of photons [20]. Further Bloch-type oscillations were predicted theoretically for interacting 1d spinor gases [21] and recently observed in an atomic Bose liquid [22]. In these settings interactions lead to the dynamical formation of periodic structures,
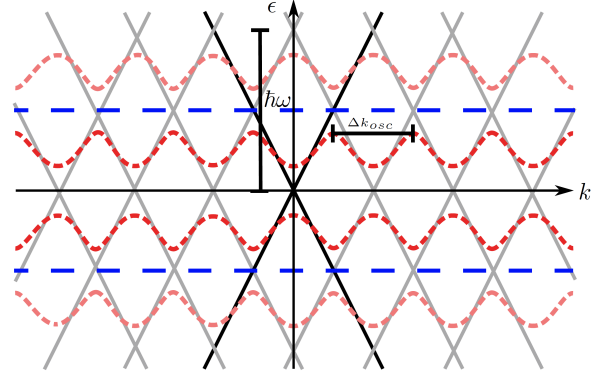

FIG. 1. Simplified scheme of the Floquet band structure $\epsilon_\pm(k)$ of a Dirac system subject to a time-periodic potential. In Floquet theory the driving (at frequency ω) introduces replicas of the original Dirac cone $E_\pm = \pm\hbar v_F k$ (black), vertically shifted in energy by multiples of $\hbar\omega$ (thin gray). The blue dashed lines mark the first energy unit cell. For finite driving strength the bands hybridize and gaps open at the crossings, leading to distinct (approximately) k-periodic Floquet bands (red dashed) whose local maxima are Δk_{osc} apart.

which can yield oscillations à la Bloch. They do not, however, involve external drivings, and hence are of different nature than the Floquet oscillations predicted here.

Specifically, we show that such periodic modes can emerge in spatially uniform systems governed by effective Dirac Hamiltonians, where the linear dispersion converts the energy periodicity of the Floquet spectrum into approximately k-periodic bands. Moreover, Floquet oscillations offer a possibility to directly image the Floquet quasi-band structure. Interestingly, they additionally exhibit Zitterbewegung features. We support our predictions by numerical calculations for two experimentally relevant prototypes of external driving, a periodic pulse sequence and circularly polarized radiation.

Consider a system $H_0(\mathbf{k})$ (with momentum operator $\mathbf{k}$) subject to a time-periodic driving $V_T(t)$ with period

T and frequency $\omega = 2\pi/T$ described by the Hamiltonian

$$H(\mathbf{k}, t) = H_0(\mathbf{k}) + V_T(t) = H(\mathbf{k}, t + T). \quad (1)$$

Via Floquet theory [23–25] the problem is transformed to finding the quasi-energy eigenvalues $\epsilon(\mathbf{k})$ of the Floquet Hamiltonian $\mathcal{H}_F(\mathbf{k}) = H(\mathbf{k}, t) - i\hbar\frac{\partial}{\partial t}$. The quasi-energies $\epsilon(\mathbf{k})$ extend to infinity in $\mathbf{k}$-space in absence of a spatial lattice. In energy, however, they are periodic in $\hbar\omega$ forming a sequence of Floquet replicas with equivalent physical properties.

For the undriven system we take an (effective) two-dimensional Dirac Hamiltonian $H_0(\mathbf{k}) = \hbar v_F \mathbf{k} \cdot \boldsymbol{\sigma}$, with constant Fermi velocity v_F and $\boldsymbol{\sigma} = (\sigma_x, \sigma_y)$ the vector of Pauli matrices. The spectrum of $H_0(\mathbf{k})$ is composed of two energy branches $E_\alpha = E_\pm = \pm\hbar v_F k$ with $k = |\mathbf{k}|$. The Floquet bands $\varepsilon_\pm$ that emerge when adding the time-periodic driving $V_T(t)$ to the system are sketched in Fig. 1. The bare Dirac cone $E_\alpha = E_\pm$ (black) is accompanied by a mesh of intersecting replicas (gray) arising from its repetition with energy period $\hbar\omega$ (in the limit of infinitely small driving $V_T(t)$). The blue dashed lines mark the corresponding first Brillouin zone (BZ) in energy. For finite $V_T(t)$ band gaps open at replica crossings and separated Floquet bands emerge (red dashed curves, see Suppl. Mat. [26]). They are approximately k-periodic due to the underlying linear (Dirac) dispersion, implying particularly pronounced Floquet oscillations, in close analogy to Bloch oscillations [27].

To gain insight into the Bloch and Floquet oscillation dynamics let us be definite and consider the time evolution of a wave packet (WP) of Dirac electrons under the influence of an additional, constant electric field $\mathbf{E} = E\mathbf{e}_x$. Here we consider the 1d motion along the field direction, generalizations to higher dimensions are straightforward. Due to the drift potential $V(x) = -eEx$, $e > 0$, the WP is accelerated and its initial wave vector k_i changes linearly in time [18]:

$$k(t) = k_i - (eE/\hbar)t. \quad (2)$$

For ordinary Bloch bands, the BZ with period $\Delta k_{osc} = 2\pi/a$ (with a the lattice constant) is traversed in the time $T_B = 2\pi/(a|eE|\hbar)$. While crossing the BZ a charge carrier changes its velocity according to the change in slope of the k-periodic band structure, leading to a Bloch oscillation in $k(t)$ with frequency $\omega_B = 2\pi/T_B$.

For Floquet systems the velocity operator is given by $\hat{v} = d\mathcal{H}_F/dk$ [18]. The diagonal terms of a WP's velocity read $\langle \hat{v}_{\alpha\alpha} \rangle = v_{\alpha\alpha} = d\epsilon_\alpha/dk$ and the corresponding position expectation value $\langle \hat{x}_{\alpha\alpha} \rangle = x_{\alpha\alpha}$ is obtained by time integration of $v_{\alpha\alpha}$. Using Eq. (2) this can be substituted by an integration over k leading to

$$x_{\alpha\alpha}(k(t)) = \frac{\hbar}{eE} \left[\epsilon_\alpha(k(t)) - \epsilon_\alpha(k_i) \right]. \quad (3)$$

These diagonal contributions to $\langle \hat{x} \rangle(t)$ already encode features of the Floquet band structure into the WP position. In particular, analogously to conventional Bloch

oscillations, the WP is expected to perform oscillations for Floquet bands similar to the ones sketched in Fig. 1 (red dashed lines).

During one (Floquet) oscillation k changes by the period Δk_{osc} of the Floquet bands (Fig. 1). Hence, Eq. (2) implies the corresponding period $T_F = (\hbar/|eE|)\Delta k_{osc}$. Due to the linear dispersion $E_\pm(k) = \pm\hbar v_F k$, we have $\hbar v_F \Delta k_{osc} = \hbar\omega$ so that the Floquet oscillation period reads

$$T_F = \frac{\hbar\omega}{v_F|eE|}. \quad (4)$$

T_F is proportional to the *inverse* period $1/T = \omega/(2\pi)$ of the driving in Eq. (1). While its analogue, the Bloch period T_B, is determined by the inverse (super-)lattice constant $1/a$, usually fixed in experiment, T_F can be tuned through ω in a range such that $T_F > T$.

In the following we consider two representative types of driving well suited to generate Floquet oscillations: a periodic sequence of short pulses and a circularly polarized light field. For the first driving protocol we use

$$V_T(t) = \sum_{l=1}^{\infty} \Theta(t - (lT - \Delta t))\Theta(lT - t)\, M\sigma_z \quad (5)$$

in Eq. (1) (with Heaviside function Θ and Pauli matrix σ_z). This pulse train periodically couples the two branches of the Dirac Hamiltonian $H_0(\mathbf{k})$ by opening a mass gap of strength M and duration Δt, see lower inset in Fig. 2(a). The resulting Floquet spectrum can be tuned either by M or by the ratio $\Delta t/T$. To be definite we choose the normalized pulse strength $M/\hbar\omega = 4.4/\pi$ and $\Delta t/T = 0.09$. The resulting Floquet band structure for this representative set of parameters is shown in Fig. 2(a). The driving opens a sequence of gaps around $\epsilon = 0$ at the intersections of the original Dirac spectrum and its replicas. A detailed analysis of these Floquet bands and the k-dependence of the gaps is given in the Suppl. Mat. [26].

A WP with initial quasi-energy and wave number as marked by the blue dot in the zoomed in area in Fig. 2(a) (red box, $k_i v_F/\omega = 0.25$) will undergo Floquet oscillations (blue arrows) when driven through the bands by a static electric field $E < 0$ such that k increases in time. Notably, since the Floquet band maxima and hence the band width vary over k-space, the resulting Floquet oscillation is expected to change its amplitude but not its frequency. In our simulations we choose the field strength E such that, according to Eq. (4), $T_F/T = 2\pi\hbar/T^2 v_F|eE| \simeq 20.8\pi$. We took initially Gaussian WPs of the form

$$\tilde{\Psi}(k, 0) = \sqrt{\frac{1}{\sqrt{\pi}\Delta k}} \exp\left(-\frac{1}{2\Delta k^2}(k - \bar{k})^2 \right) \cdot \begin{pmatrix} 1 \\ 1 \end{pmatrix}, \quad (6)$$

with width Δk and central mode $\bar{k}$. We employ two complementary approaches to compute and analyze Floquet
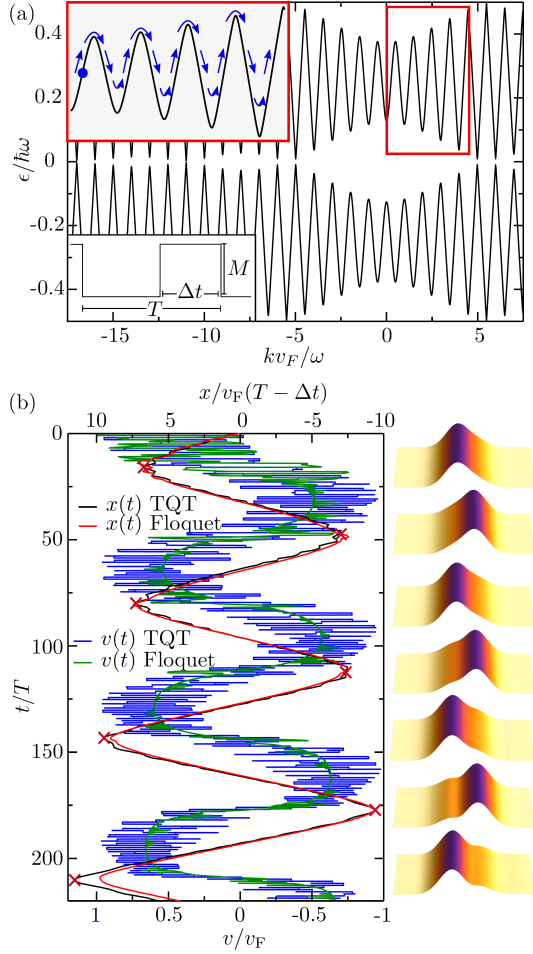
FIG. 2. Floquet oscillations in a driven, spatially homogeneous Dirac system. (a) Floquet bands from a periodically opened mass gap (see Eq. (5) and lower left inset for the pulse shape) with band gaps at the intersections of the unperturbed Dirac cones and their replicas (as sketched in Fig. 1). Two separated bands emerge in the energy window $\hbar\omega$. The motion of a WP (with initial position indicated by the blue dot) due to a static electric field is sketched by the blue arrows in the zoomed-in region framed in red. (b) Left panel: Simulations of the WP position and velocity expectation values based on direct time evolution (TQT) and Floquet theory (see text for details). The numerical results mirror the characteristic shape of the Floquet band structure, further showing Zitterbewegung signatures. Right panel: Snapshots of the WP in position space (extended to 2d for better visualization) taken at times marked as red crosses in the left panel.

oscillations: Floquet theory and direct time-integration of the full time-dependent effective Dirac equation including the **E**-field.

To compute the WP velocity within Floquet theory we start from Ehrenfest's theorem

$$v(t) = \langle \hat{v}(t) \rangle = \frac{i}{\hbar} \langle \Psi(t) | [H(t), \hat{x}] | \Psi(t) \rangle, \qquad (7)$$

where $[H(t), \hat{x}] = -i\hbar v_F \sigma_x$ for the Dirac case. $|\Psi(t)\rangle$

is obtained via the time evolution operator of a Floquet system [28] that for a single k-mode reads

$$U_k(t,0) = \sum_{\alpha=\pm} \exp\left(-\frac{i}{\hbar}\epsilon_\alpha(k)t\right) |\phi_{\alpha,k}(t)\rangle\langle\phi_{\alpha,k}(0)|. \quad (8)$$

Here ϵ_α are the Floquet quasi-energies and $|\phi_{\alpha,k}(t)\rangle$ the corresponding eigenstates of $\mathcal{H}_F$, including replicas $n\hbar\omega$ (see Eq. (13) in the Suppl. Mat. [26]), each consisting of two branches $\alpha = \pm$ from the linear dispersion. The additional electric field induces a linear change of k, which we account for by adjusting $k(t)$ according to Eq. (2). Applying $U_k(t,0)$ to an initial (WP) state $|\Psi(0)\rangle = \sum_{k_i} c_{\alpha,k_i} |\phi_{\alpha,k_i}(0)\rangle$, where $|c_{\alpha,k_i}|^2 = |\langle\phi_{\alpha,k_i}(0)|\Psi(0)\rangle|^2$ describes the initial occupation of branch α, and plugging Eq. (8) into Eq. (7) gives

$$v(t) = v_F \sum_{k_i} \sum_{\alpha,\beta=\pm} c^*_{\alpha,k_i} c_{\beta,k_i} \langle\phi_{\alpha,k(t)}(t)|\sigma_x|\phi_{\beta,k(t)}(t)\rangle$$
$$\times \exp\left(-\frac{i}{\hbar}\left[\epsilon_\beta\left(k(t)\right) - \epsilon_\alpha\left(k(t)\right)\right]t\right). \quad (9)$$

Here $k(t)$ is given by Eq. (2). The occupation $|c_{\alpha,k_i}|^2$ is time-independent as long as different Floquet bands are far enough apart for Landau-Zener inter-band transitions [29–34] to be neglected. This is the case for the time scales $t \leq 200T$ considered below.

For the periodic pulse sequence, Eq. (5), we numerically compute $v(t)$ by means of Eq. (9) and $x(t) = \int_0^t \mathrm{d}t'v(t')$. Due to the rectangular pulse shape we must include up to $n = 500$ Floquet modes to achieve sufficient convergence. The results are shown in the left panel of Fig. 2(b) as red and green lines for $x(t)$ and $v(t)$, respectively. They indeed show distinct Floquet oscillations, as predicted, with period $T_F \simeq 20.5\pi T$, matching the expected value $T_F \simeq 20.8\pi T$ from Eq. (4).

The off-diagonal velocity term ($\alpha \neq \beta$) in Eq. (9) encodes the interference of states living in different Floquet bands, giving rise to an additional feature, Zitterbewegung [35, 36] caused by the Floquet Dirac band structure (see Suppl. Mat. [26]).

Our second, complementary method to compute Floquet oscillations is based on the WP propagation algorithm "Time-dependent Quantum Transport" (TQT) [37]. The WP is discretized on a rectangular grid and the time evolution operator for the full Hamiltonian including the drift field, $H(t) = H_0(\mathbf{k}) + V_T(t) - Ex$, is computed. Then the Lanczos method [38] is used to evaluate the action of the time evolution operator on the WP and to compute $\Psi(x,t)$. Time-dependent position and velocity expectation values are then calculated through $x(t) = \langle\hat{x}(t)\rangle = \int |\Psi(x,t)|^2 x\,\mathrm{d}x$ and $v(t) = \langle\hat{v}(t)\rangle = \frac{\mathrm{d}}{\mathrm{d}t}\langle\hat{x}(t)\rangle$. The resulting TQT data is shown in Fig. 2(b), left panel, as black and blue curves for $x(t)$ and $v(t)$, respectively. They approximately coincide with those computed within Floquet theory, also showing Zitterbewegung on top of the Floquet oscillations.

Moreover, the WP position $x(t)$ computed with TQT precisely reflects characteristic features of the Floquet quasi bands, shown in the red box in Fig. 2(a), namely the increasing amplitude and the sharpening of the maxima and minima although TQT directly integrates the time-dependent Schrödinger equation without using Floquet formalism.

While the static electric drift field enters into the full Hamiltonian governing the numerically exact TQT time evolution, within the Floquet approach its effect is included via the acceleration theorem (2) into the time evolution, Eqs. (8, 9). The latter approximation, together with residual numerical errors from the cutoff in the Floquet quantum number, could explain the slight deviations between Floquet and TQT data in the left panel of Fig. 2(b).

Finally, in the right panel of Fig. 2(b) we present snapshots of the absolute square $|\Psi(x, t)|^2$ taken at the turning points (marked as red crosses) of the red curve in the left panel. They show clear-cut Floquet oscillations of the full WP in configuration space generated for the setting of a periodic pulse sequence.

The experimental realization of Floquet oscillations could be easier to achieve in in an alternative setup, employing circularly polarized light as periodic driving. The associated vector potential $\mathbf{A}$ enters (linearly) the Dirac Hamiltonian (1) via the minimal coupling

$$V_T(t) = \mathbf{A}(t) \cdot \boldsymbol{\sigma} = A \begin{pmatrix} \cos(\omega t) \\ \sin(\omega t) \end{pmatrix} \cdot \boldsymbol{\sigma}. \qquad (10)$$

The Floquet quasi-bands of graphene illuminated by circularly polarized light have already been studied extensively [39–42]. Recently, also transport [43] and topological [44–47] properties were investigated. Instead, here we focus on generating Floquet oscillations for realistic experimental parameters. To be closer to measurements, we explicitly treat the 2d case with an initial, radially symmetric Gaussian WP analogously to Eq. (6). Using again TQT we simulate the WP dynamics in presence of the electric field $\mathbf{E} = E\mathbf{e}_x$. In contrast to the periodically opened mass gap, the light field changes the wave vector in the representation of the time-dependent Hamiltonian.

We calculate the Floquet band structure and the WP dynamics for two different dimensionless driving strengths $\tilde{A} = v_F eA/(\hbar\omega)$ to demonstrate the field amplitude influence on the Floquet oscillation frequency. Figure 3(a) shows that the Floquet oscillation period given by Eq. (4) works for driving strengths $\tilde{A} < 0.9$ (black curve), i.e. as long as the induced band gap at $k = 0$ is smaller than the energy BZ. For strong driving $\tilde{A} > 0.9$ the Floquet band is instead distorted (red curve).

As shown in Fig. 3(b), our TQT simulations of the position expectation values of two WPs with scaled initial momenta $k_i v_F/\omega = -1.57$ and -0.64 for $\tilde{A} = 0.5$ and 1.1, respectively (marked by blue dots in panel (a)) again clearly show Floquet oscillations, nicely reflecting
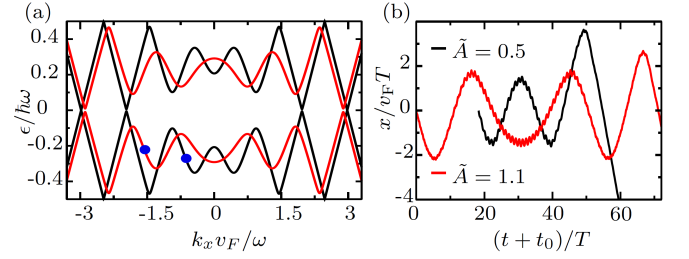

FIG. 3. (a) Floquet bands of a Dirac system illuminated with circularly polarized light with scaled amplitude $\tilde{A} = 0.5$ (black curves) and 1.1 (red curves). (b) Floquet oscillations: Mean position of a WP driven through the bands shown in (a) starting with momenta k_i marked as blue dots in (a). The initial time t_0 for the black curve is shifted to $t_0/T = 18.26$ to highlight the close connection to the Floquet band structure of panel (a).

the shape of the underlying Floquet band structure as expected. Since the gaps between unperturbed Dirac cones open in a smaller k-range than for the periodic pulse train (5), there are less cycles of regular Floquet oscillations. At longer times Landau-Zener transitions to neighboring Floquet bands substantially alter the WP motion.

The above analysis and simulations constitute a proof of principle for generating Floquet oscillations in systems with an effective Dirac dispersion. Concerning possible experimental realizations, graphene [48] and topological insulators [49, 50] appear suitable. Other effective Dirac systems, e.g. for plasmons [51] or polaritons [52], could also be considered, provided an effective accelerating ("electric") field can be realized. The radiation frequency ω must be chosen such that the Floquet BZ lies in the energy range governed by the linear dispersion. Additionally, $\omega > \omega_F \gg 1/\tau$ is required, where τ denotes a typical relaxation time of charge carriers in the given system. Regarding graphene, realizations for charge carriers in real [48] monolayer graphene or cold atoms in artificial [53] honeycomb lattices seem both feasible. The latter has the advantages that one can additionally tune v_F entering the Floquet frequency and that relaxation through interaction effects can be avoided. As a rough estimate for graphene, to achieve a circularly polarized light field strength corresponding to $\tilde{A} \simeq 0.5$ and assuming radiation with frequency 10 THz, the according moderate intensity yields $I = \frac{c\epsilon_0}{2}A^2\omega^2 \simeq 0.1 \frac{\text{kW}}{\text{cm}^2}$, where c is the speed of light and ϵ_0 the vacuum permittivity. Then an electric field $E \simeq 0.1 \frac{\text{kV}}{\text{cm}}$ is sufficient to generate Floquet oscillations of frequency $\omega_F \gtrsim 2$ THz. Since this value is larger than the inverse transport relaxation times $1/\tau = 0.05 - 1$ THz obtained in hexagonal boron nitride-encapsulated graphene [54, 55], Floquet oscillations could in principle be observed in such systems. This could open an alternative way to generate THz radiation [56, 57].

To conclude we showed that free particles in a static electric drift field and obeying a linear Dirac-type dis-

person can perform spatially periodic motion, Floquet oscillations, when subject to time-periodic driving. The Floquet time lattice takes the role of the spatial lattice required for conventional Bloch oscillations. Such Floquet oscillations feature Zitterbewegung and characteristic amplitude modulations that could provide a tool to experimentally map the Floquet quasi-bands. A closer consideration of Landau-Zener transitions between different Floquet bands and the question how the topology of Floquet bands[14] is reflected in corresponding Floquet oscillations opens interesting perspectives for future research.

—————

* klaus.richter@physik.uni-regensburg.de

[1] F. Bloch, Zeitschrift für Physik **52**, 555 (1929).

[2] C. Zener, Proceedings of the Royal Society of London A: Mathematical, Physical and Engineering Sciences **145**, 523 (1934).

[3] For a review see A. Wacker, Physics Reports **357**, 1 (2002).

[4] For an early proposal to employ superlattices see L. Keldysh, Soviet Physics-Solid State **4**, 1658 (1963).

[5] J. Feldmann, K. Leo, J. Shah, D. A. B. Miller, J. E. Cunningham, T. Meier, G. von Plessen, A. Schulze, P. Thomas, and S. Schmitt-Rink, Phys. Rev. B **46**, 7252 (1992).

[6] C. Waschke, H. G. Roskos, R. Schwedler, K. Leo, H. Kurz, and K. Köhler, Phys. Rev. Lett. **70**, 3319 (1993).

[7] A. A. Ignatov, E. Schomburg, K. F. Renk, W. Schatz, J. F. Palmier, and F. Mollot, Annalen der Physik **506**, 137 (1994).

[8] M. Ben Dahan, E. Peik, J. Reichel, Y. Castin, and C. Salomon, Phys. Rev. Lett. **76**, 4508 (1996).

[9] S. R. Wilkinson, C. F. Bharucha, K. W. Madison, Q. Niu, and M. G. Raizen, Phys. Rev. Lett. **76**, 4512 (1996).

[10] T. Pertsch, P. Dannberg, W. Elflein, A. Bräuer, and F. Lederer, Phys. Rev. Lett. **83**, 4752 (1999).

[11] R. Morandotti, U. Peschel, J. S. Aitchison, H. S. Eisenberg, and Y. Silberberg, Phys. Rev. Lett. **83**, 4756 (1999).

[12] H. Sanchis-Alepuz, Y. A. Kosevich, and J. Sánchez-Dehesa, Phys. Rev. Lett. **98**, 134301 (2007).

[13] O. Schubert, M. Hohenleutner, F. Langer, B. Urbanek, C. Lange, U. Huttner, D. Golde, T. Meier, M. Kira, S. W. Koch, and R. Huber, Nature Photonics **8**, 119 (2014).

[14] N. H. Lindner, G. Refael, and V. Galitski, Nature Physics **7**, 490 (2011).

[15] C. J. Fujiwara, K. Singh, Z. A. Geiger, R. Senaratne, S. V. Rajagopal, M. Lipatov, and D. M. Weld, Phys. Rev. Lett. **122**, 010402 (2019).

[16] Alberti A., Ivanov V. V., Tino G. M., and Ferrari G., Nature Physics **5**, 547 (2009).

[17] E. Haller, R. Hart, M. J. Mark, J. G. Danzl, L. Reichsöllner, and H.-C. Nägerl, Phys. Rev. Lett. **104**, 200403 (2010).

[18] S. Arlinghaus and M. Holthaus, Phys. Rev. B **84**, 054301 (2011).

[19] K. Kudo and T. S. Monteiro, Phys. Rev. A **83**, 053627 (2011).

[20] L. Yuan and S. Fan, Optica **3**, 1014 (2016).

[21] D. M. Gangardt and A. Kamenev, Phys. Rev. Lett. **102**, 070402 (2009).

[22] F. Meinert, M. Knap, E. Kirilov, K. Jag-Lauber, M. B. Zvonarev, E. Demler, and H.-C. Nägerl, Science **356**, 945 (2017).

[23] G. Floquet, Annales scientifiques de l'École Normale Supérieure **12**, 47 (1883).

[24] E. Ince, *Ordinary Differential Equations* (Dover Publication, 1956).

[25] W. Magnus and S. Winkler, *Hill's Equation*, Dover Books on Mathematics Series (Dover Publications, 2004).

[26] See Supplemental Material for a general introduction to Floquet theory, the discussion of Floquet bands of a Dirac system with a periodically opened mass gap, and a discussion of Zitterbewegung in Floquet bands.

[27] General nonlinear dispersions $\epsilon_\alpha(k)$, *e.g.* two hyperbolic branches, give rise to sequences of intersections that are not equidistant in k and thereby deny a constant Floquet oscillation period.

[28] P. Hänggi, in *Quantum Transport and Dissipation* (Wiley-vch, 1998).

[29] L. Landau, Phys. Z. Sowjetunion **2**, 118 (1932).

[30] C. Zener, Proceedings of the Royal Society of London A: Mathematical, Physical and Engineering Sciences **137**, 696 (1932).

[31] L. Landau, Phys. Z. Sowjetunion **1**, 88 (1932).

[32] E. K. G. Stueckelberg, *Theorie der unelastischen Stösse zwischen Atomen* (Birkhäuser, 1933).

[33] B. M. Breid, D. Witthaut, and H. J. Korsch, New Journal of Physics **8**, 110 (2006).

[34] V. Krueckl and K. Richter, Phys. Rev. B **85**, 115433 (2012).

[35] E. Schrödinger, *Ueber die kraeftefreie Bewegung in der relativistischen Quantenmechanik* (Akademie der wissenschaften in kommission bei W. de Gruyter u. Company, 1930).

[36] W. Zawadzki and T. M. Rusin, Journal of Physics: Condensed Matter **23**, 143201 (2011).

[37] V. Krückl, *Wave packets in mesoscopic systems: From time-dependent dynamics to transport phenomena in graphene and topological insulators*, Ph.D. thesis (2013).

[38] C. Lanczos, J. Res. Natl. Bur. Stand. B **45**, 255 (1950).

[39] T. Oka and H. Aoki, Phys. Rev. B **79**, 081406 (2009).

[40] O. V. Kibis, Phys. Rev. B **81**, 165433 (2010).

[41] Y. Zhou and M. W. Wu, Phys. Rev. B **83**, 245436 (2011).

[42] S. E. Savel'ev and A. S. Alexandrov, Phys. Rev. B **84**, 035428 (2011).

[43] J. Atteia, J. H. Bardarson, and J. Cayssol, Phys. Rev. B **96**, 245404 (2017).

[44] H. K. Kelardeh, V. Apalkov, and M. I. Stockman, Phys. Rev. B **93**, 155434 (2016).

[45] P. Delplace, Á. Gómez-León, and G. Platero, Phys. Rev. B **88**, 245422 (2013).

[46] G. Usaj, P. M. Perez-Piskunow, L. E. F. Foa Torres, and

C. A. Balseiro, Phys. Rev. B **90**, 115423 (2014).

[47] P. M. Perez-Piskunow, L. E. F. Foa Torres, and G. Usaj, Phys. Rev. A **91**, 043625 (2015).

[48] A. H. Castro Neto, F. Guinea, N. M. R. Peres, K. S. Novoselov, and A. K. Geim, Rev. Mod. Phys. **81**, 109 (2009).

[49] M. Z. Hasan and C. L. Kane, Rev. Mod. Phys. **82**, 3045 (2010).

[50] X.-L. Qi and S.-C. Zhang, Rev. Mod. Phys. **83**, 1057 (2011).

[51] G. Weick, C. Woollacott, W. L. Barnes, O. Hess, and E. Mariani, Phys. Rev. Lett. **110**, 106801 (2013).

[52] T. Jacqmin, I. Carusotto, I. Sagnes, M. Abbarchi, D. D. Solnyshkov, G. Malpuech, E. Galopin, A. Lemaître, J. Bloch, and A. Amo, Phys. Rev. Lett. **112**, 116402 (2014).

[53] L. Tarruell, D. Greif, T. Uehlinger, G. Jotzu, and T. Esslinger, Nature **483**, 302 (2012).

[54] L. Wang, I. Meric, P. Y. Huang, Q. Gao, Y. Gao, H. Tran, T. Taniguchi, K. Watanabe, L. M. Campos, D. A. Muller, J. Guo, P. Kim, J. Hone, K. L. Shepard, and C. R. Dean, Science **342**, 614 (2013).

[55] A. I. Berdyugin, S. G. Xu, F. M. D. Pellegrino, R. Krishna Kumar, A. Principi, I. Torre, M. Ben Shalom, T. Taniguchi, K. Watanabe, I. V. Grigorieva, M. Polini, A. K. Geim, and D. A. Bandurin, Science **364**, 162 (2019).

[56] S. Ganichev and W. Prettl, *Intense Terahertz Excitation of Semiconductors* (Oxford University Press, 2005).

[57] R. A. Lewis, Journal of Physics D: Applied Physics **47**, 374001 (2014).

[58] J. H. Shirley, Phys. Rev. **138**, B979 (1965).

[59] H. Sambe, Phys. Rev. A **7**, 2203 (1973).

[60] P. Reck, C. Gorini, A. Goussev, V. Krueckl, M. Fink, and K. Richter, Phys. Rev. B **95**, 165421 (2017).

[61] E. Schrödinger, Sitz. Press. Akad. Wiss. Phys.-Math. **42**, 418 (1930).

[62] J. Schliemann, D. Loss, and R. M. Westervelt, Phys. Rev. Lett. **94**, 206801 (2005).

[63] R. Gerritsma, G. Kirchmair, F. Zahringer, E. Solano, R. Blatt, and C. F. Roos, Nature **463**, 68 (2010).

[64] W. Zawadzki and T. M. Rusin, Journal of Physics: Condensed Matter **23**, 143201 (2011).

[65] C. Qu, C. Hamner, M. Gong, C. Zhang, and P. Engels, Phys. Rev. A **88**, 021604 (2013).

[66] L. J. LeBlanc, M. C. Beeler, K. Jimnez-Garca, A. R. Perry, S. Sugawa, R. A. Williams, and I. B. Spielman, New Journal of Physics **15**, 073011 (2013).

Supplemental material to the paper
"Floquet oscillations in periodically driven Dirac systems"

Vanessa Junk,[1] Phillipp Reck,[1] Cosimo Gorini,[1] and Klaus Richter[1]

[1]*Institut für Theoretische Physik, Universität Regensburg, D-93040 Regensburg, Germany*

BASIC RELATIONS IN FLOQUET THEORY

In the following we describe how to obtain the Floquet band structure for a finite driving strength $V_T(t)$ without the electric field, which is later included by a shift of k when computing Floquet oscillations. Generally, the Floquet operator $\mathcal{H}_F$ is given by

$$\mathcal{H}_F = H_0(\mathbf{k}) + V_T(t) - i\hbar\partial_t, \tag{11}$$

where $H_0(\mathbf{k})$ is the Hamiltonian of the time-independent system. Since the eigenstates of $\mathcal{H}_F$, $\Phi_\alpha(\mathbf{k},t)$, are periodic in time, they can be expanded in a Fourier series:

$$\Phi_\alpha(\mathbf{k},t) = \sum_{n=-\infty}^{\infty} \mathbf{u}_\alpha(\mathbf{k},n)e^{in\omega t}. \tag{12}$$

The dimension of the coefficients $\mathbf{u}_\alpha(\mathbf{k},n)$ is equal to the number of branches α of the time-independent Hamiltonian $H_0(\mathbf{k})$, i. e. two in our case. In order to find these coefficients and the corresponding eigenenergies ϵ_α, the Floquet equation (11) is multiplied by $e^{-im\omega t}$, $m \in \mathbb{Z}$, and averaged over one period T to end up with [58, 59]

$$\sum_{n=-\infty}^{\infty} \underbrace{(\mathcal{H}_{0F,mn}(\mathbf{k}) + V_{F,mn})}_{\mathcal{H}_{F,mn}(\mathbf{k})} \mathbf{u}_\alpha(\mathbf{k},n)$$
$$= \epsilon_\alpha(\mathbf{k})\mathbf{u}_\alpha(\mathbf{k},m). \tag{13}$$

Here the contributions from $V_T(t)$ are denoted by $V_{F,mn}$ and the contributions from $H_0(\mathbf{k})$ and $-i\hbar\partial_t$ by $\mathcal{H}_{0F,mn}(\mathbf{k})$. Note that the resulting eigenvalue problem is time-independent and all the dynamics of a wave packet in the system are incorporated in the Floquet basis states [18]. To account for this when projecting a wave packet from the time-dependent basis to the Floquet basis, the relation $\langle k_o(t)\rangle_t = k_{Floquet}$ is used, where $\langle k_o(t)\rangle_t = \frac{1}{T}\int_0^T k_o(t)\,\mathrm{d}t$. The time dependence of $k_o(t)$ is introduced by the time-periodic driving $V_T(t)$. Hereafter, we refer to $k_{Floquet}$ when talking of wave numbers and suppress its subscript to simplify the notation. The Floquet Hamiltonian without coupling

$$\mathcal{H}_{0F,mn}(\mathbf{k}) = (\hbar v_F \mathbf{k}\cdot\boldsymbol{\sigma} + m\hbar\omega)\delta_{mn} \tag{14}$$

is diagonal and describes the Dirac bandstructure shown in Fig. 1. The driving Hamiltonian

$$V_{F,mn} = \frac{1}{T}\int_0^T \mathrm{d}t\, V_T(t)e^{i(n-m)\omega t} \tag{15}$$

on the other hand couples different Floquet modes $\mathbf{u}_\alpha(\mathbf{k},n)$ and thus can lead to the opening of band gaps in the originally linear spectrum (see Fig. 1). For the numerical evaluation, the resulting infinite matrix $\mathcal{H}_F$ has to be truncated at a finite value $\pm n$ that corresponds to the number of Floquet replicas taken into account. When performing numerical calculations, one has to make sure that the results are converged for the chosen value of n.

FLOQUET QUASI-BAND STRUCTURE OF A DIRAC SYSTEM WITH PERIODICALLY OPENED MASS GAP

Here we give a more detailed analysis of the Floquet band structure of a Dirac system with a periodically opened mass gap. The potential describing this time-dependent pulsing is given in Eq. (5). For the mass gap, we find with Eq. (15)

$$V_{F,mn} = \frac{M}{2\pi i(n-m)}\left(1 - e^{-2\pi i(n-m)\frac{\Delta t}{T}}\right)\sigma_z. \tag{16}$$

Qualitatively, the two time scales Δt and T involved are reflected in k-space. While the longer scale T makes for the high-frequency oscillations of the Floquet bands due to the replicas, the smaller time scale Δt is responsible for the slow modulation, i.e. the different gap sizes as function of k shown in Fig. 4.

On a more quantitative level, the dependence of the Floquet bands on the pulse amplitude M and pulse duration Δt can be best understood when studying the influence of one pulse on a wave packet in the static Dirac cone. This has been done extensively in Ref. [60] and will only be summarized here. Let us consider a wave packet initially occupying states in the upper cone. The opening and closing of the gap causes a redistribution of the wave packet to both cones, leading to a new superposition state. The amplitude of the part now occupying the other cone - in our example the lower one - can easily be calculated analytically [60]:

$$A(k) = -\frac{i}{\sqrt{1+\eta^2}}\sin\left(\mu\sqrt{1+\eta^2}\right), \tag{17}$$

where $\eta = E_{k,\pm}/M$ and $\mu = M\Delta t/\hbar$. This transition amplitude only depends on the initial energy $E_{k,\pm}$ of the state and the pulse parameters. A numerical comparison of the corresponding transition probability $P(k) = |A(k)|^2$ and the Floquet band structure reveals that the gaps that open at the intersections of the repetitions of the original cone are directly related to the
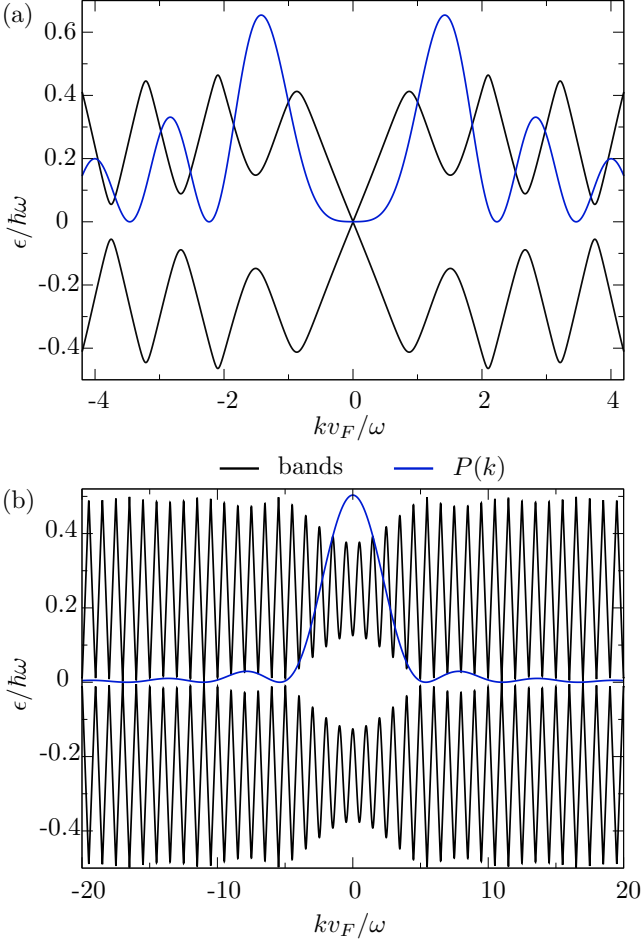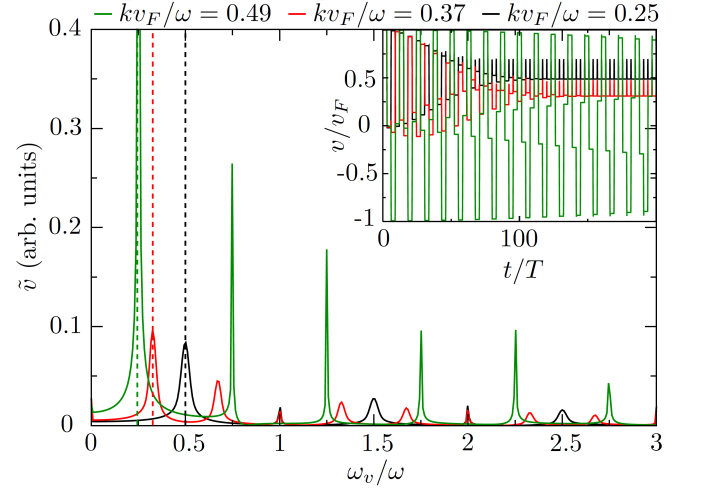
FIG. 5. Frequency analysis by a Fourier transform of the velocity $\tilde{v}(\omega_v)$ of wave packets with different $\bar{k}$. Since no electric field is applied, k is constant. The dashed lines mark ω_{ZB} as expected from Eq. (18) which match perfectly the numerically obtained peaks. The inset shows the corresponding time-dependency of the velocities. For the Fourier analysis, the respective average velocities have been subtracted to avoid a zero-frequency peak.

FIG. 4. Floquet band structure (black curves) and corresponding transition probability $P(k)$ (blue) for (a) $\mu = 6.3$, $\Delta t/T = 0.5$ and (b) $\mu = 0.4$, $\Delta t/T = 0.09$. The bands shown in Fig. 2(a) of the main paper are a zoom into those depicted in panel (b). For both parameter sets one can easily see that the gap in the Floquet bands closes whenever $P(k)$ goes to zero.

transition probability at that k-value: The larger $P(k)$, the larger the band gap. The reason for this dependence can be motivated in the following way. $P(k)$ describes for a single pulse the proportion of the wave packet that is transferred to the other band, i.e. how much a single pulse couples upper and lower band of the Dirac cone. On the other hand, the band gap of the Floquet bands is due to this coupling of (initially) linear band replicas. Therefore, it is not surprising that $P(k)$ and the band gap width are directly related.

We show this for two exemplary band structures in Fig. 4. In panel (a) we set $\mu = 6.3$ and $\Delta t/T = 0.5$. Since $P(k) = 0$ around $k v_F/\omega = 0$ the original Dirac cone is preserved. For larger k band gaps open. The resulting complex band structure is a perfect example of how nicely the Floquet band structure can be tuned based on the transition probability $P(k)$. The band structure shown

in panel (b) is the same as the one shown in Fig. 2(a) of the main paper bur for a larger range of k-values. There, a wide area around $k v_F/\omega = 0$ is gapped. For an appropriate choice of parameters (as in panel (b)) a large k-window, in which Landau-Zener transitions are suppressed, can be chosen to support Floquet oscillations.

ZITTERBEWEGUNG IN A DIRAC SYSTEM WITH PERIODICALLY OPENED MASS GAP

Zitterbewegung (ZB) was originally predicted by Schrödinger for the Dirac equation [61] but an analogue is also visible in multiband systems [62–66]. The reason is the interference of particle and antiparticle contributions in a wave packet, or respectively the contributions of different bands, in cases when the velocity operator does not commute with the Hamiltonian. The corresponding term is the offdiagonal term of the expectation value of the velocity operator and the frequency is given by the difference of the energies. In our case, we also have an effective two band model due to the Floquet bands with an offdiagonal term of the velocity as seen in Eq. (9). The frequency of the corresponding "Floquet Zitterbewegung" is given by the energy gap between the two Floquet quasi-energies,

$$\omega_{ZB} = (\epsilon_\beta(k) - \epsilon_\alpha(k))/\hbar. \tag{18}$$

In Fig. 5 we show the Fourier transform $\tilde{v}(\omega_v)$ of the

velocity of a wave packet starting at different k-values in the Floquet band structure to analyze the frequency spectrum. We denote the variable of the Fourier transform of the velocity by ω_v. For these calculations no static electric field was applied, such that k and therefore ω_{ZB} stay constant in time. Before performing the Fourier transform to investigate the frequency of the oscillations, the mean velocity value was subtracted of the corresponding data to avoid a peak at $\omega_v = 0$.

The dashed lines mark ω_{ZB} as calculated by Eq. (18).

Their good agreement with the spectrum confirms that the off-diagonal velocity in the Floquet picture describes ZB caused by the interference of states occupying different Floquet bands. Since the velocity has a rectangular shape, the peaks are repeated at higher harmonics. This rectangular shape can be explained in our example by the fact that the velocity can only change during the mass gap, which means that the harmonic oscillation of the ZB is effectively sampled with the driving frequency ω.